

Optical Sub-System Design Considerations for Multi-Beam Photocathode

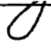
Timothy N. Thomas

B.S. Mechanical Engineering, Portland State University, 1995



A thesis presented to the faculty of the
Oregon Graduate Institute of Science and Technology
in partial fulfillment of the
requirement for the degree
Master of Science
in
Electrical and Computer Engineering

March 23, 2000

The thesis "Optical Sub-System Design Considerations for Multi-Beam Photocathode" by Timothy N. Thomas has been examined and approved by the following Examination Committee:

C. Neil Berglund 
Professor

Dan Hammerstrom
E.C.E. Department Head

 Jack McCarthy 
Assistant Professor

ACKNOWLEDGMENTS

The author thanks his wife McKevin for her understanding and support during the many months of working evenings and weekends to complete this work. The author also thanks Paul Allen, Professor C. Neil Berglund, Suresh Gosavi, Joel Johnson, Professor Bill Mackie, Professor Jack McCarthy, and Xiaolan Chen for their invaluable contributions. Thanks also to Etec Corporation and the United States Defense Advanced Research Projects Agency for supporting this work.

TABLE OF CONTENTS

Abstract.....	vi
INTRODUCTION	3
1.1 Laser System.....	3
1.2 2-Beam Light Optics Module	3
1.2.1 2-Beam Light Optics Module Beam Path	4
1.3 Focusing Light Optics Objective Lens	6
1.4 Photocathode Vacuum Chamber.....	6
1.5 Video System.....	7
2.1 Final Assembly.....	9
2.2 Light Optics Beam Spacing Adjustment.....	10
3.1 Calibration and Emission.....	14
3.2 Emission Limitations.....	16
3.3 Two Beam Emission	16
4.1 Summary	18

LIST OF FIGURES

<i>Number</i>	<i>Page</i>
Figure 1-1 Two-Beam Light Optics Module beam path.....	4
Figure 1-2 Two-Beam Light Optics Module with associated mechanical hardware.	5
Figure 1-3 Photocathode Vacuum Chamber.....	7
Figure 2-1 Final assembled test station.....	9
Figure 2-2 Displacement through a tilted plain-parallel window of thickness t.....	10
Figure 2-3 2-Beam Light Optic Module beam displacement gear geometry.....	10
Figure 2-4 Laser beam displacement as a function of rack-gear displacement.....	12
Figure 2-5 Linear performance over entire photocathode field size.....	13
Figure 3-1 CAD file of patterned photocathode. Dimensions are in μm . Dimensioned areas are electron emission areas.	14
Figure 3-2a Photo-emission of patterned photocathode. White areas are electron emission zones.	15
Figure 3-2b Output of video system. Profile shown is for the vertical line drawn through Figure 3-2a. Horizontal scale is approximately $2 \mu\text{m}$ per division.....	16
Figure 3-3a Simultaneous emission of two electron beams as a result of photo-emissive photocathode illuminated with two laser beams.	17
Figure 3-3b Spot profiles of spots shown in Figure 3-3a. Spot size at photocathode is approximately $5 \mu\text{m}$ FWHM.....	17

Abstract

OPTICAL SUB-SYSTEM DESIGN CONSIDERATIONS FOR MULTI-BEAM PHOTOCATHODE

by Timothy N. Thomas

Supervising Professor: C. Neil Berglund

An apparatus for studying the interaction of two electron beams has been constructed. Generation of two electron beams is achieved by illuminating a photocathode with two separate, 1 μm diameter laser beams. The design and method of producing the two laser beams that are used to illuminate the photocathode will be discussed. A vacuum chamber with electron optics for imaging the photocathode emission on to a YAG scintillator will be described. A CCD video system used to image the YAG emission will also be reviewed. These sub-system components act together as a system to permit real-time study of how one electron source effects another in spot profile, size, and position. The system described has the ability to precisely control the separation of the two laser beams symmetrically about the electron optical axis, the ability to independently shutter each beam, and the ability to adjust the relative brightness of one beam to the other.

Chapter 1

INTRODUCTION

As the density of features found on semiconductor devices increases, the difficulty in creating these features becomes more complex. Smaller feature sizes require more complicated processes and lithography equipment. The throughput of single-beam raster-scanning lithography systems (1)[Rieger, et al, 1988] begins to slow as the feature sizes become smaller. Increasing the number of write beams in the lithography system is one way to regain some of the throughput lost.

Laser beam based raster-scanned lithography systems are able to increase the number of write beams by splitting the main beam in to the required number of beamlets. This increases the throughput of the system but this approach is limited to the features sizes that can be created using light as the exposing source. The wavelength of the source and the method used to concentrate the light source at the final image plane produces fundamental limitations in feature resolution.

Electron beam raster-scanned lithography systems are able to produce spot sizes at the final image plane which are significantly smaller than light based systems. The single writing beam of a conventional electron beam lithography system is able to create small and detailed features but has throughput limitations because of the single beam.

Multiple electron beams can be created by illuminating a photoemissive material (2)[Berglund, et al, 1964] with multiple light beams. A vacuum-mounted photocathode can be fabricated from photo-electric materials. The photocathode can be a window that is transparent to light with the photo-electric material applied to optimize electron emission for the given material and light wavelength. Such a photocathode was created for testing in this work.

Illuminating the photocathode with multiple focused laser beams produces the desired multiple electron beam emission. The laser light wavelength must exceed the work function of the photo-electric material deposited on the photocathode surface.

Many parameters must be experimentally measured to study the result of illuminating a photocathode surface with multiple laser beams and the resulting multiple electron beams. These include the interaction between the electron beams as a function of beam separation, photocathode heating as a result of light absorption, and photocathode heating affects as a result of multiple laser beams.

The purpose of this work is to develop an apparatus that is useful for studying the behavior of a multiple beam photocathode.

The photocathode consists of a thin metal film deposited on a glass substrate and is illuminated by a wavelength of light that exceeds the work function of the metal film. The photocathode is mounted in a vacuum in such a way that the electrons that are emitted from the metal film can be collected and imaged on to a YAG scintillating screen. Multiple electron beams are created by illuminating the photocathode with multiple light beams. The light beams are created by careful splitting of a laser beam. The laser source delivers the required photon energy level to exceed the work function of the metal film on the photocathode. In this paper, the metal film is a 15 nm thick layer of gold and the laser wavelength is 257 nm. The total system is comprised of four major components. These are the laser, the module which splits the laser beam, the photocathode vacuum chamber, and a video system for viewing the YAG emission.

1.1 Laser System

The light source for the apparatus is a Coherent Corporation I300 FreD laser. The laser is an argon-ion gas laser tuned with a Littrow prism to lase at 514 nm. The 514 nm continuous wave output is delivered to a frequency doubling section within the laser to produce the final output of 257 nm. The non-linear optical material and the design of the frequency doubling section of the laser causes the beam to propagate as a near-Gaussian beam in one axis and a sinc² function in the other. Significant ellipticity is also present in the main beam. The laser is capable of delivering more than 250 mW of power but is only certified to operate at 100 mW.

1.2 2-Beam Light Optics Module

The laser output is delivered to the light optics module by three mirrors. The mirrors are used to elevate the laser output to the correct height from the optical table to provide the necessary degrees of adjustment to satisfy the alignment requirements of the 2-Beam Light Optic Module.

1.2.1 2-Beam Light Optics Module Beam Path

The laser light enters the two-beam light optics module (Fig. 1-1 and 1-2) at the $\frac{1}{2}$ wave retardation plate (WP1) and polarizing beamsplitting cube (PB1).

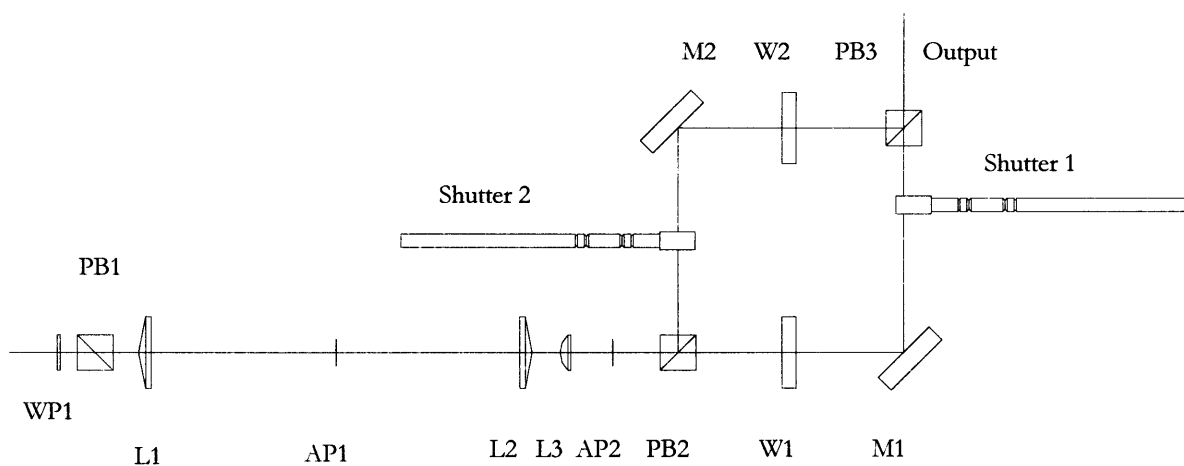


Figure 1-1 Two-Beam Light Optics Module beam path.

WP1 and PB1 can be rotated about the optical axis to either adjust the overall intensity the module output or to balance the beam intensities. The plano-convex lenses L1 and L2 have the same focal length. L1 images the laser input on to the face of a 30 μm diameter aperture (AP1). AP1 is heavily overfilled by the incoming laser beam. This eliminates the sinc^2 lobes and ellipticity present on the raw laser beam. This technique produces severe diffraction which propagates in the far-field to produce a Newton ring pattern. L2 collects the output of AP1 and nearly collimates it for delivery to the focusing plano-convex lens L3. L3 focuses the beam through a 15 μm diameter aperture (AP2) to remove the Newton rings. A polarizing

beamsplitter (PB2) then splits the beam in to two separate beams. The beam which is transmitted through PB2 enters a simple 6 mm thick window (W1) and passes on to a fold mirror (M1) which directs the beam toward a shutter (Shutter 1) and another polarizing beamsplitter (PB3) which serves to combine the two beams. The output of PB3 is delivered to an objective lens which will be discussed later. The portion of light that is reflected by PB2 passes toward Shutter 2 and is reflected by another fold mirror (M2). The light reflected from M2 passes through another simple window (W2) and enters PB3 where it is reflected and exits the module. W1 and W2 are mounted in bearings and driven by precision gears with micrometer precision in such a way that they rotate about the point of incidence on the front face in equal and opposite directions. This adjustment provides the ability to control the separation between the two beams as a result of refraction through the tilted windows. Shutter 1 and Shutter 2 simply serve as manual shutters to enable zero, one, or two beams to exit the module. Figure 1-2 illustrates the completed module with the associated mechanical mounts.

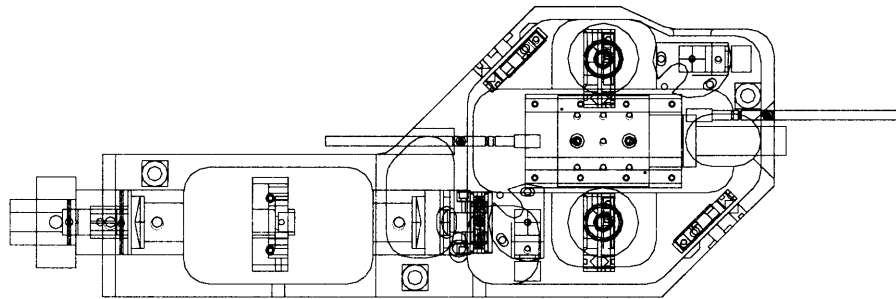


Figure 1-2 Two-Beam Light Optics Module with associated mechanical hardware.

1.3 Focusing Light Optics Objective Lens

A custom, double-Gauss objective lens was fabricated to produce the required 1 μm diameter spots with a field size of 100 μm on the photocathode gold film. The objective lens has to produce an acceptable image through the 6 mm thick photocathode substrate and have a sufficient track-length to allow adequate safety clearance between the Two-Beam Light Module and the 10 kV potential of the photocathode. The objective lens has minimal field distortion to minimize the light optic contribution when studying electron beam interactions.

1.4 Photocathode Vacuum Chamber

The photocathode is a 6 mm thick window which serves as a vacuum break as well as a photocathode. The photocathode forms a seal with the vacuum chamber (Fig. 1-3) through the compression of an o-ring. The vacuum side of the photocathode window is coated with a thin-film layer of material, which will be tested for its electron emission properties. For this paper, Au was deposited with an approximate thickness of 15 nm. The photocathode material is fused-silica but can be made of other materials to provide better thermal performance.

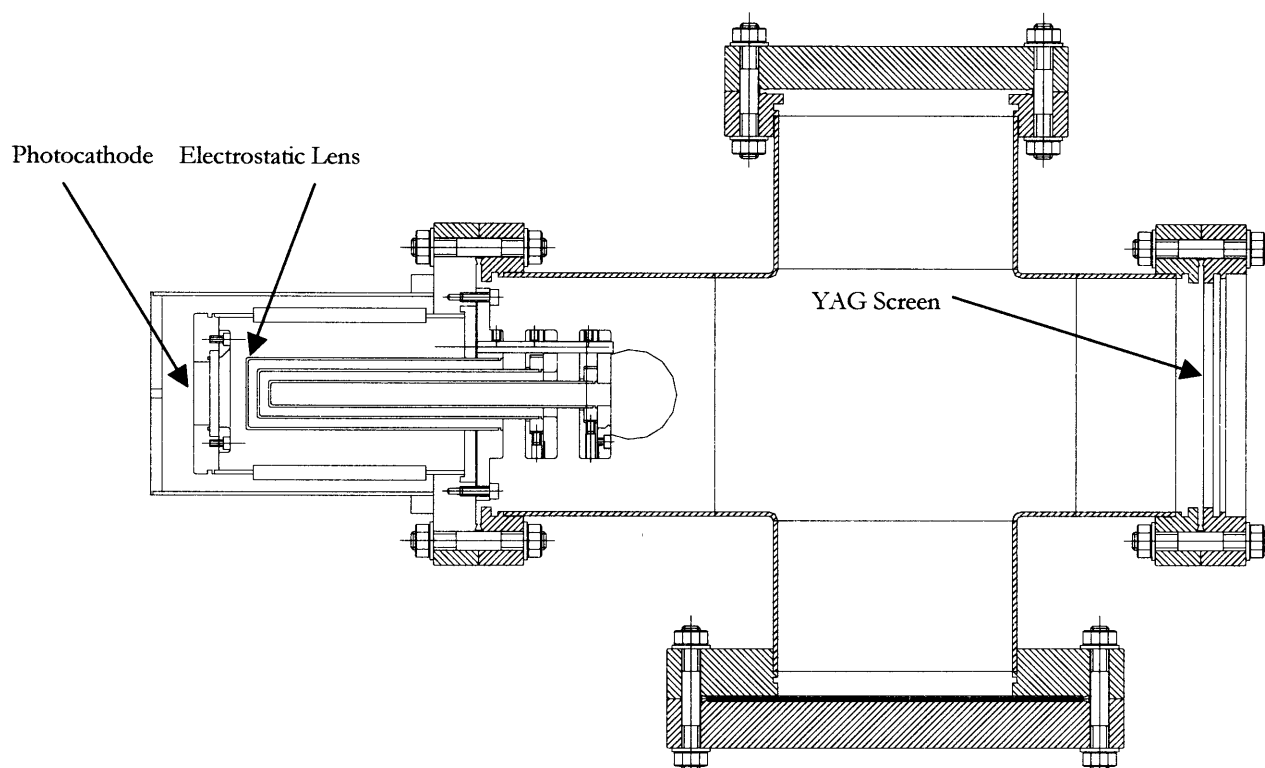


Figure 1-3 Photocathode Vacuum Chamber

The electrostatic lens collects the electrons and images them on to the face of an Al coated YAG scintillating screen. The magnification of the electron optics is approximately 20. For a $1\ \mu\text{m}$ diameter laser beam on the photocathode metal film a $20\ \mu\text{m}$ diameter spot should be produced at the YAG screen.

1.5 Video System

The video system is comprised of a scientific black & white CCD camera, lens, computer, image capture card, and image analysis software. The CCD camera lens has a magnification of approximately 2.5. The output of the camera can be view real time on the computer monitor. Images are stored and analyzed with the software. The software can determine the separation

between spots and spot profile. These parameters can be monitored as the separation between the laser beams is adjusted or if one laser beam is shuttered.

Chapter 2

2.1 Final Assembly

The 2-Beam Light Optic Module is shown in figure 2-1 with the laser and vacuum chamber. The 2-Beam Light Optic Module is shown on a riser plate to elevate the module to the proper height to match the vacuum chamber elevation. Three 45 degree fold mirror near the output end of the laser are used to align the laser to the input of the 2-Beam Light Optic Module.

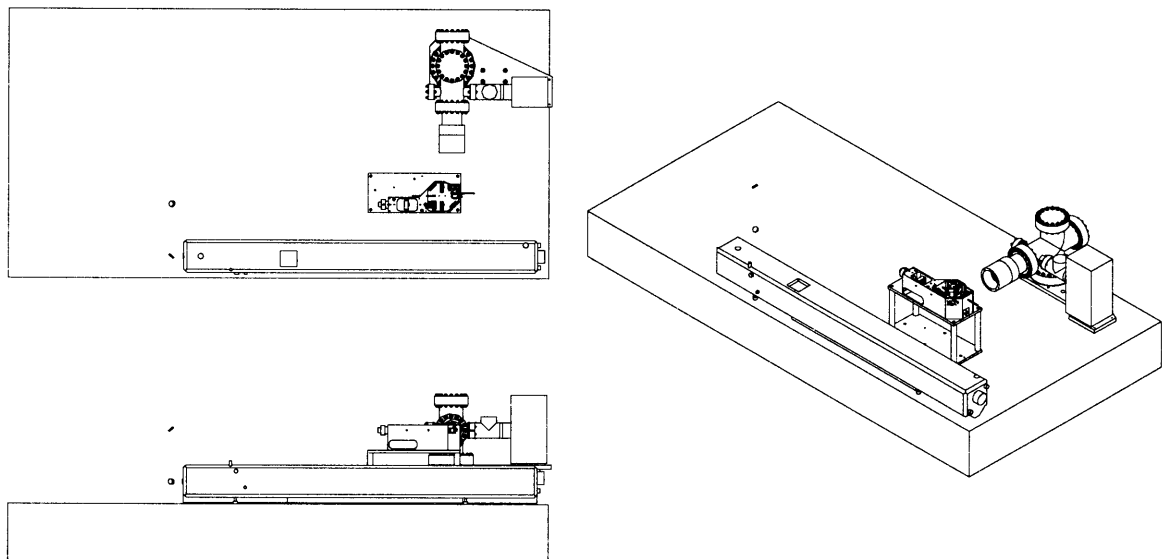


Figure 2-1 Final assembled test station.

2.2 Light Optics Beam Spacing Adjustment

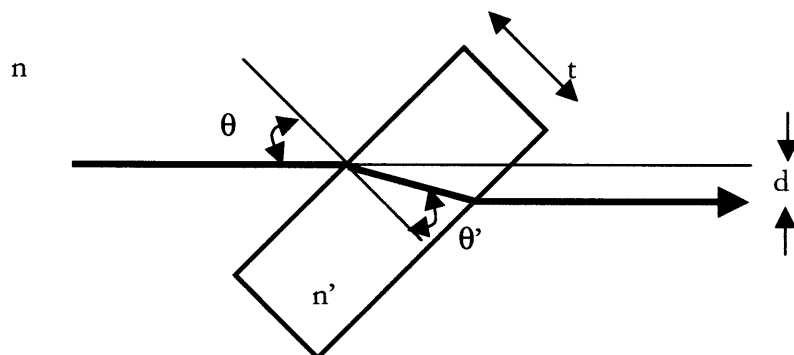


Figure 2-2 Displacement through a tilted plain-parallel window of thickness t .

Each of the two beams within the Two-Beam Light Optic Module can be displaced according to Figure 2-2 above. Changing the separation between the two laser beams will change the separation between the two electron beams emitted from the photocathode. Tilting a window will produce a well understood displacement of the laser beam and will make it possible to study the properties of the emitted electron beams as their separation changes. The amount of tilt applied to the window, θ , is determined by the radius of the mechanical gear of which the center of rotation is about the front surface of the window. The mechanical gear is driven by a mechanical rack gear which is driven by a micrometer.

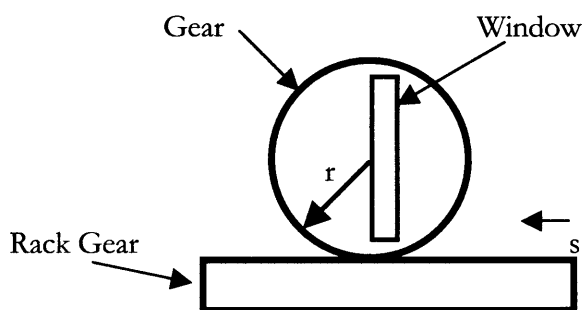


Figure 2-3 2-Beam Light Optic Module beam displacement gear geometry.

The gear has a radius, r , as shown in Fig. 2-3. Moving the rack gear a displacement s will cause the gear to rotate an angle β as given by,

$$\beta = \frac{s}{r} \text{ eqn. 2.1}$$

For convenience, in degrees,

$$\theta = \frac{s}{r} \left(\frac{180 \text{ deg}}{\pi \text{ radian}} \right) \text{ eqn. 2.2}$$

The angle θ' is determined using Snell's Law,

$$n \sin \theta = n' \sin \theta' \text{ eqn. 2.3}$$

where n is the refractive index of air and n' is the refractive index of the window at the laser wavelength of 257 nm. For fused silica n' is approximately 1.47. Continuing the refraction process through the plate to the output side the displacement can be found to be,

$$d = t \cos \theta (\tan \theta - \tan \theta') \text{ eqn. 2.4}$$

Solving equation 2.3 for θ' and substituting in to the equation 2.4 yields,

$$d = t \cos \theta \left(\tan \theta - \tan \left(\sin^{-1} \left(\frac{n \sin \theta}{n'} \right) \right) \right) \text{ eqn. 2.5}$$

For the Two-Beam Light Optic Module, the mechanical gear radius is 17.197 mm. Using this value and plotting equation 2.5 yields the graph shown in Figure 2-4.

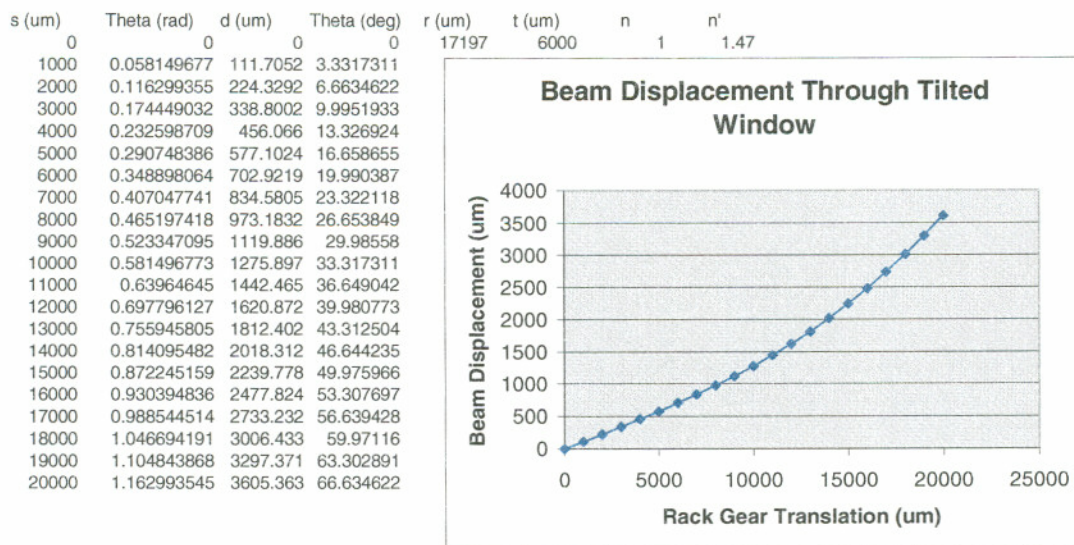


Figure 2-4 Laser beam displacement as a function of rack-gear displacement.

Figure 2-4 clearly shows the displacement is not linear for large gear displacement. The field size out of the light optic reduction lens is only $100\ \mu\text{m}$. The reduction demagnification produced by the reduction lens is approximately 10X. To achieve full field separation of the laser beams at the photocathode each window would be tilted to produce $50\ \mu\text{m}$ at the photocathode image plane. Given the 10X demagnification, this would require the window to be tilted to produce a displacement after the window of $500\ \mu\text{m}$. For such a small displacement, the result is almost perfect linear adjustment as shown in Figure 2.5.

s (um)	Theta (rad)	d (um)	r (um)	t (um)	n	n'	
0		0	0	17197	6000	1	1.47
1000	0.058149677	111.7052					
2000	0.116299355	224.3292					
3000	0.174449032	338.8002					
4000	0.232598709	456.066					
5000	0.290748386	577.1024					
6000	0.348898064	702.9219					
7000	0.407047741	834.5805					
8000	0.465197418	973.1832					
9000	0.523347095	1119.886					
10000	0.581496773	1275.897					
11000	0.63964645	1442.465					
12000	0.697796127	1620.872					
13000	0.755945805	1812.402					
14000	0.814095482	2018.312					
15000	0.872245159	2239.778					
16000	0.930394836	2477.824					
17000	0.988544514	2733.232					
18000	1.046694191	3006.433					
19000	1.104843868	3297.371					
20000	1.162993545	3605.363					

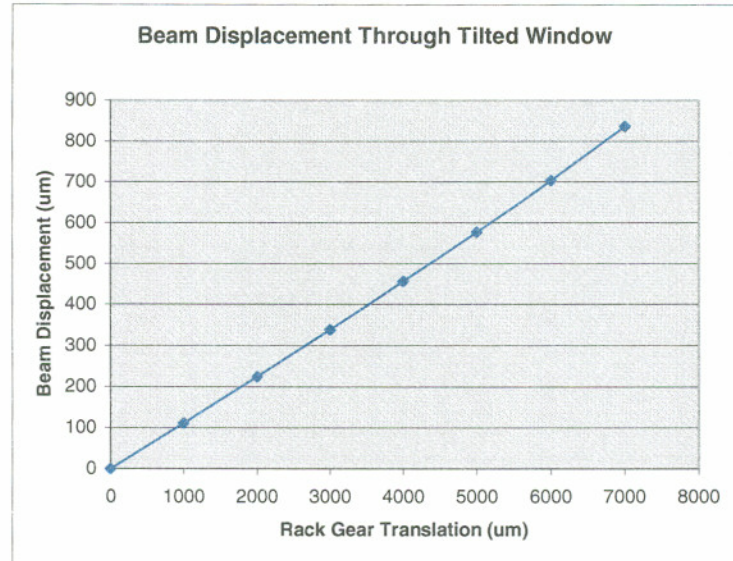


Figure 2-5 Linear performance over entire photocathode field size.

Chapter 3

3.1 Calibration and Emission

The real magnification of the electron and video camera optics is initially unknown. The magnification was determined by generating a patterned photocathode. The patterned photocathode was created from a 6 mm thick fused silica stepper mask with the pattern shown in Figure 3-1.

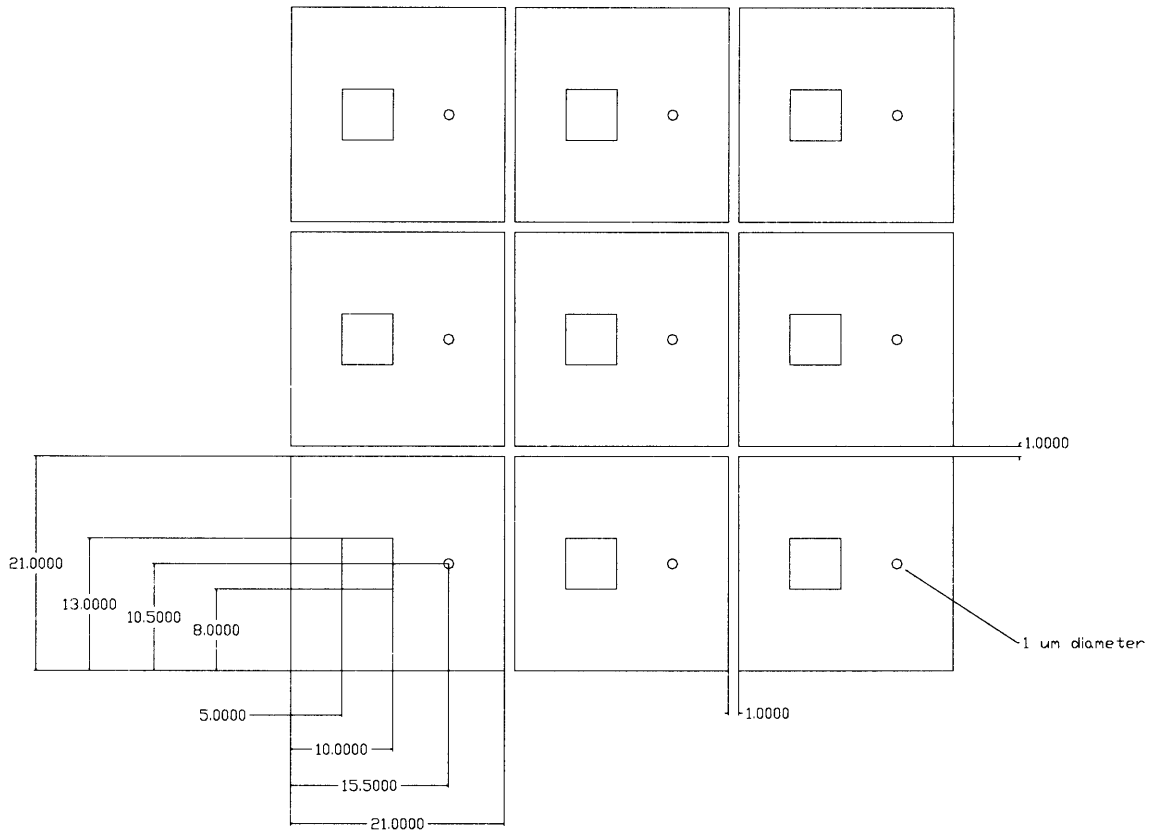


Figure 3-1 CAD file of patterned photocathode. Dimensions are in μm . Dimensioned areas are electron emission areas.

The stepper mask has a conventional chrome coating which is approximately 100 nm thick. After exposure, etching, and stripping of the photoresist the pattern shown in Figure 3-1 remains on the mask as zones that are clear of chrome. The entire mask is coated with 15 nm of gold to create a photo-emission layer in the zones which are free of chrome. The distance between each feature and the size of each feature is accurately measured prior to applying the gold. After mounting in the vacuum chamber the photocathode is flood illuminated with the raw laser beam to fully illuminate the active area of the photocathode. The electron optics produce an image of the photocathode emission at the YAG screen. The video system captures the YAG emission. From the video image the number of CCD camera pixels between features on the YAG screen can be counted to determine the magnification of the electron optics and the video optics. Figure 3-2a illustrates the output of the YAG scintillator as seen by the video camera with the flood illuminated photocathode in place.

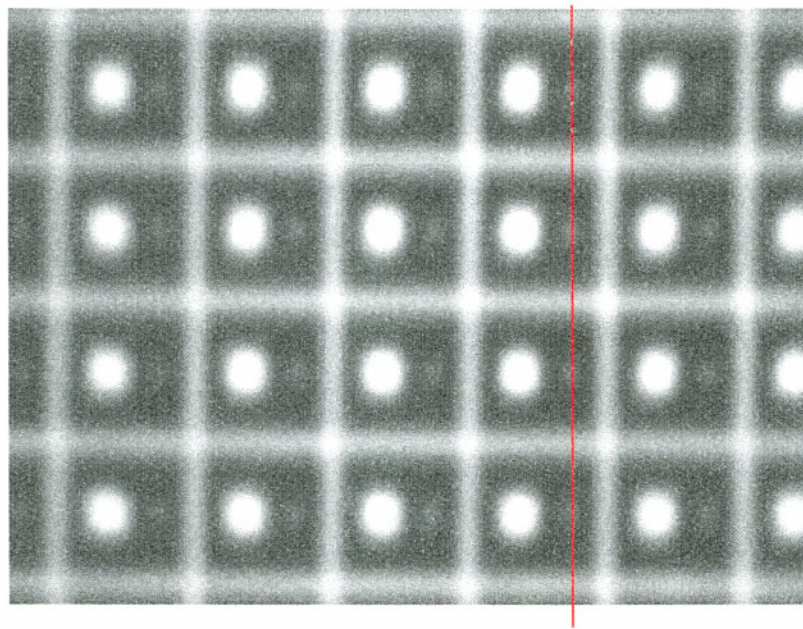


Figure 3-2a Photo-emission of patterned photocathode. White areas are electron emission zones.

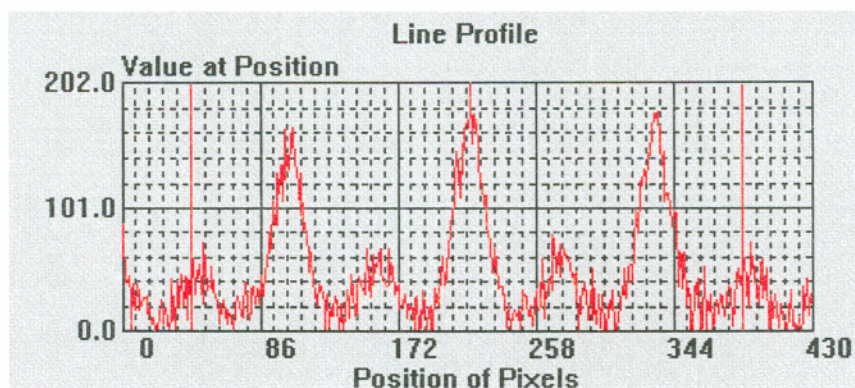


Figure 3-2b Output of video system. Profile shown is for the vertical line drawn through Figure 3-2a. Horizontal scale is approximately $2 \mu\text{m}$ per division.

3.2 Emission Limitations

From Figure 3-2a it is apparent that the $1 \mu\text{m}$ wide lines are heavily blurred and the $1 \mu\text{m}$ contact on the photocathode surface is not fully resolved. This is a result of aberrations within the electron optics. The electron optics used for this study consist of a simple electrostatic lens without the aid of aberration correction found on more complicated electron optics systems. In addition, strong magnetic fields developed by the electromagnet surrounding the DUV laser tube severely influenced the output of the electron optics. Future work will involve implementing μ -metal shields to reduce the magnetic fields near the vacuum chamber.

3.3 Two Beam Emission

With the calibration of the electron and video optics complete determining the spot size of the laser beam at the photocathode surface is possible, provided the spot size of the laser beam is greater than the resolution limit of the electron optics. As stated in the previous section, it was not possible to resolve $1 \mu\text{m}$ laser spots at the photocathode as a result of system aberrations. Figure 3-3a illustrates the best two-beam emission obtained.

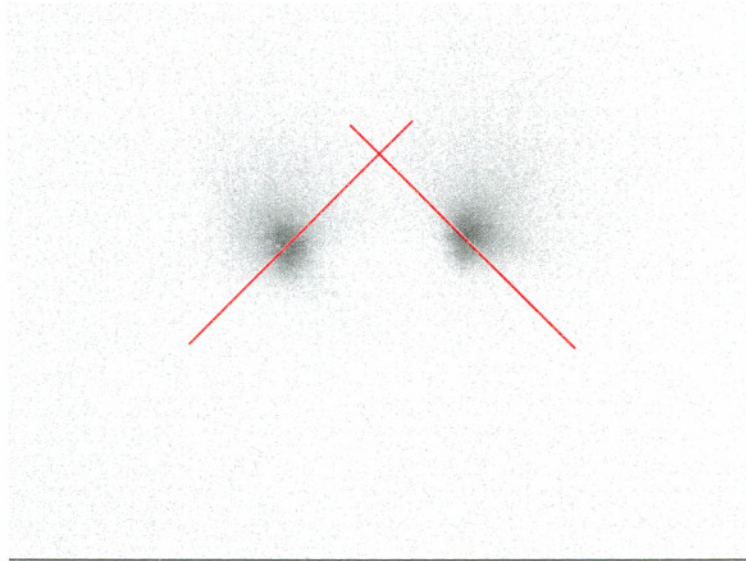


Figure 3-3a Simultaneous emission of two electron beams as a result of photo-emissive photocathode illuminated with two laser beams. (YAG screen)

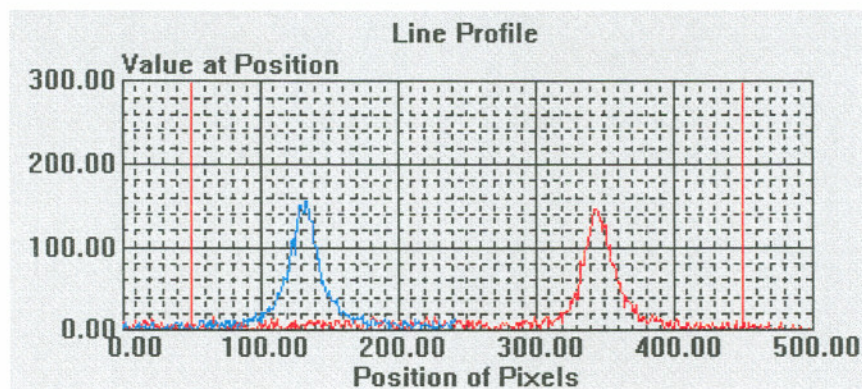


Figure 3-3b Spot profiles of spots shown in Figure 3-3a. Spot size at photocathode is approximately $5\ \mu\text{m}$ FWHM.

The separation between the electron beams shown in figure 3-3a varies when the 2-Beam Light Optic Module windows are rotated. It is possible to adjust the separation of the two beams while observing the video output in real-time. It was possible to change the separation between the beams from 0 to $100\ \mu\text{m}$ (as measured at the photocathode surface).

It was also possible to adjust the relative intensity of each one beam to the other by adjusting the retardation plate.

Chapter 4

4.1 Summary

Construction of an apparatus for studying the interaction of two electron beams has been completed. The system has been calibrated and all adjustments have been verified to work properly. The system is unable to resolve 1 μm spot sizes at the photocathode as a result of uncorrected aberrations of the electrostatic electron optics lens system and magnetic fields generated by the laser tube. In addition, it was found through an independent Focault knife edge test that the laser spot size emitted by the Two-Beam Light Optic module is approximately 3 μm FWHM.

The larger than expected laser spot size is a result of aberrations within the reduction lens that focuses the laser light on to the photocathode surface. Improving the output of this lens is ongoing.

Etec Corporation has measured a similar laser system for magnetic field strength (3)[Mankos, 1999] and measured values of approximately 100 Gauss (DC level) near the laser head. From their measurements it is expected that the field strength in the area of the photocathode will be approximately 1 or 2 Gauss. Future work of shielding the vacuum chamber from the laser's magnetic field should reduce the aberrations produced by the electron optics.

The work of studying the interactions of two electron beams is left to future researchers.

References

-
- 1 "IMAGE QUALITY ENHANCEMENTS FOR RASTER SCAN LITHOGRAPHY," SPIE Proceedings, VOL 922, March 2-4, 1988, Page 55-64, M. Rieger, J. Schoeffel, P. Warkentin
 - 2 "PHOTOEMISSION STUDIES OF COPPER AND SILVER: THEORY," C. N. Berglund & W. E. Spicer, PHYSICAL REVIEW, Volume 136, Number 4A, Page A1030, November 16, 1964.
 - 3 Telephone conversation with Marian Mankos, Etec Corporation, Hayward, CA 1/99.